Doty

# Maximum S/N in Narrow-bore Solids - The OptiMAS$^{TM}$ Probe, with Cryogenically Cooled Critical Circuit Components (C$^5$)

Siddarth Shevgoor, George Entzminger, J. B. Spitzmesser, Leyu Li, Jennifer R. Doty,
Vince Cothran, Daniel Arcos, Jatin Kulkarni, John Staab, Laura L. Holte, and F. David Doty
Doty Scientific, Columbia, SC

## INTRODUCTION AND BACKGROUND

The primary objectives of this development of an advanced solids probes for H/X/Y MAS applications in narrow-bore (NB) magnets at the highest available fields are:

1. Maximum S/N
2. Automatic sample exchange
3. Minimum rf sample heating
4. Optimum spectral resolution
5. Optional high-performance Magic Angle Gradient (MAG) coil
6. Full-range, multi-nuclear tuning
7. Highest spinning stability and ease of use
8. $^2$H lock option on a 4th channel
9. Extended VT operation to below 100 K

**RF Efficiency.** RF circuit efficiency in a multi-resonance circuit is defined as the fraction of rf power delivered from the probe port to the sample coil and sample, since in principle all other losses should be eliminated. RF circuit efficiencies in 3 to 5 mm triple-resonance "single-coil" MAS probes at very high fields are typically in the range of 25-35% at the low frequency (LF) and 15-40% at the mid-frequency (MF). While higher efficiencies on all channels have been achieved using a cross-coil for $^1$H and a solenoid for the MF and LF, they are still generally in the range of 30-50% for both the LF and the MF. Such low efficiencies suggests there is considerable opportunity for noise reduction. Cooling the tuning elements external to the sample coil improves circuit efficiency (by improving their Qs), and it improves S/N even more than expected just on the basis of improved rf efficiency by reducing the noise temperature of these resistances.

**S/N in Cryo-circuits.** The principle of reciprocity states that the sensitivity in receiving an NMR signal (in a coil and sample at room temperature) is proportional to the "efficiency" of generating the rf $B_1$ by the receiver coil during the transmit pulse. This may be expressed mathematically as:

$$S/N \propto \frac{B_1 V_S}{\sqrt{P_T}} \propto \frac{V_S}{t_{90}\sqrt{P_T}} \quad , \qquad (1)$$

where $P_T$ is the rf power needed to generate the rotating rf field $B_1$ or the 90-degree pulse of length $t_{90}$ within the sample volume $V_S$.

The above simplification of the principle of reciprocity understates the S/N advantage of cryo-probes because it assumes the noise voltage is simply proportional to the square root of resistances (coil, capacitors, leads, sample, shields) within the circuit, whereas in fact noise voltage is proportional to $(RT)^{1/2}$, where $T$ is the temperature.

Cryogenic cooling of the sample coil in a VT MAS probe appears impractical in the NB magnet. However, cryogenic cooling of the critical LF/MF circuit components other than the sample coil is practical, and this promises potential of up to 50% increase in S/N.

Equation (1) is easily extended to handle complex circuits where various losses are at different temperatures as follows:

$$S/N \propto \frac{B_1 V_S}{\sqrt{\sum P_n T_n}} \ , \qquad (2)$$

where $P_n$ is the transmit power dissipated in the nth resistance of temperature $T_n$ when generating $B_1$, and the sum is over all resistances (in coils, capacitors, and leads) in the circuit. The easiest way to show this is to transform each loss into an equivalent resistor $R_n$ in series with the sample coil. Then the noise voltage contribution from each resistor is proportional to $(R_n T_n)^{1/2}$, and its contribution to noise power (assuming Q>>1) is proportional to $R_n T_n / R_P$, where $R_P$ is the equivalent parallel resistance of the coil circuit, which is a constant in the summation. The contribution of $R_n$ to transmitter power, on the other hand, is simply proportional to $R_n$.

Approaching the S/N limits in triple-resonance MAS. It is important to appreciate that there is a very wide range for S/N in high-field triple-tuned solids probes. For example, a 900 MHz 2.5 mm probe by a major competitor achieved about 50:1 on glycine, while our **750 MHz XC4 (4 mm) achieved 220:1** on the same $^{13}$C glycine test in a narrow-bore magnet. Still, MF rf efficiency on this XC4 probe was only ~30% and the NF of the preamp with filter and cable losses was ~1.5 dB, which implies a factor of 2 gain in S/N should be possible without cooling the sample coils if the noise from the components external to the sample coils could be eliminated. The major sources of this excess noise are: circuit inductors (transmission lines or coils), circuit capacitors, cables, preamp, and filters.

In a realistic design, in which most of the more critical circuit components external to the sample coil are cooled to ~100 K, **an increase in S/N of ~70%** is predicted by the circuit simulations with a little cooling of the sample coil - though the experiments suggest somewhat higher gain may be possible. (The most critical loss that cannot be greatly reduced is in the long, flexible leads to the tuning elements.) The S/N gain is achieved more by reducing the mean noise temperature of the probe rf circuit than by increasing its Q. Hence, realizing this gain requires an ultra-low-noise preamp. With standard preamps, the gain in S/N may be under 50%.

E-PHEMT Preamps. The lowest NF is currently obtained with Enhancement mode Pseudomorphic High Electron Mobility Transistors (E-PHEMT) – a type of GaAs FET. The ATF-58143 has NFmin below 0.13 dB (at 25$^0$C) at frequencies below 500 MHz when matched at the optimum (frequency dependent) input reflection coefficient. Detailed circuit simulations show that tuned $^{13}$C E-PHEMT preamps with high-rejection stop filters for $^{15}$N and $^1$H can achieve total NF below 0.3 dB (not including cable losses) at least up to 250 MHz ($^{13}$C) without cooling. Work is currently underway to demonstrate performance at several different frequencies, including 75 MHz and 125 MHz. Preliminary results are expected within several months.

## Development of an Ultra-stable Drop-in (DI-4) Spinner Utilizing a Novel, Inflow Bernoulli Bearing

A novel inflow Bernoulli axial bearing for MAS has been developed (patent pending) that provides exceptional axial stability as well as compatibility with auto sample exchange. The classic Andrews/Beams drive/bearing design and later designs, such as those by Bartuska, Lewis, and others, have utilized outward flow in a conical space at the bottom of the rotor that establishes an axial bearing and also provides some or all of the needed drive torque for the sample spinner. However, such designs appear to have insufficient axial stability for many gradient MAS methods and some HR-MAS applications. They also do not appear to be compatible with the ultra-low-E cross-coil for $^1$H, which seems essential, both for minimal rf sample heating and for good efficiency with the long leads required for spinner flipping for auto sample exchange.

The DI-4 (4 mm rotor) spinner assembly is illustrated in **Figure 1** below.

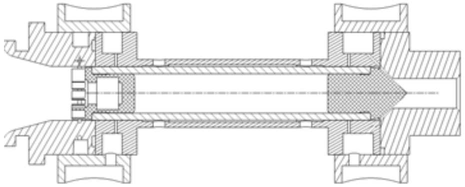

Gas is injected radially inward with a large axial rearward component and a small negative azimuthal component into the conical bearing region from its periphery near the right end in the above drawing. A self-stabilizing axial bearing may be formed with improved stability and stiffness for rotor surface speeds up to at least 80% of the speed of sound. Typical axial oscillations, measured using a linear variable displacement transducer (LVDT), are under 2 μm rms over a wide range of spinning conditions. ***This is an order of magnitude better axial stability than what has often been seen in alternative spinner designs compatible with automatic sample exchange.***

Motive power to spin the rotor is provided by a radial-inflow microturbine at the upper end (above, left) of the rotor. A combination of CFD and FEA analysis was used in the turbine and bearing optimization.

Both spinner designs are compatible with extended VT ranges, automatic sample exchange, and ***ultra-low-E cross-coils for order-of-magnitude reduction in rf sample heating***. Such cross-coils (see **Figures 3 and 4** below) require extra external access and extra rotor length compared to single solenoids.

The high axial stability and the accuracy of the magnetic compensation of the cross-coil components are confirmed in **Figure 2** below. FWHM spectral resolution better than 0.5 Hz on $^1$H, with nearly ideal lineshape, is obtained on CHCl$_3$.

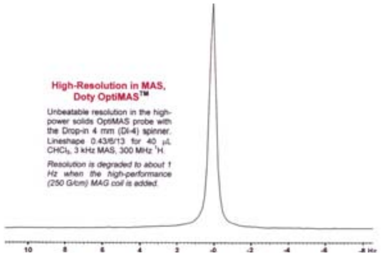
**High-Resolution in MAS, Doty OptiMAS™**

Unbeatable resolution in the high-power solids OptiMAS probe with the Drop-in 4 mm (DI-4) spinner. Lineshape 0.43/6/13 for 40 μL CHCl$_3$, 3 kHz MAS, 300 MHz $^1$H.

*Resolution is degraded to about 1 Hz when the high-performance (250 G/cm) MAG coil is added.*

The 3 mm spinner (**DI-3**) demonstrated 30 kHz MAS, and the **DI-4** achieved 23 kHz. A specialized adaptation of the 3 mm spinner with a zirconia dewar between the rotor and the rf coils is being used in our CryoMAS probe to permit sample temperatures well above RT while the rf coils are at cryogenic temperatures.

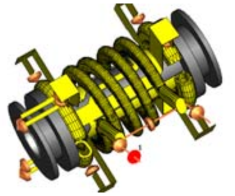

Figure 3. The $^1$H XC and the LF/MF solenoid are shown here as simulated in CST MWS 5.0. The capacitors (8 for tuning, plus feed and balance) are represented by chamfered disks.

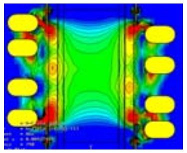

Figure 4. Plot with 2.5% contours of the $^1$H $B_1$ magnitude in the YZ plane for the XC with a saline sample at 750 MHz. The outer solenoid is not driven at the high frequency.

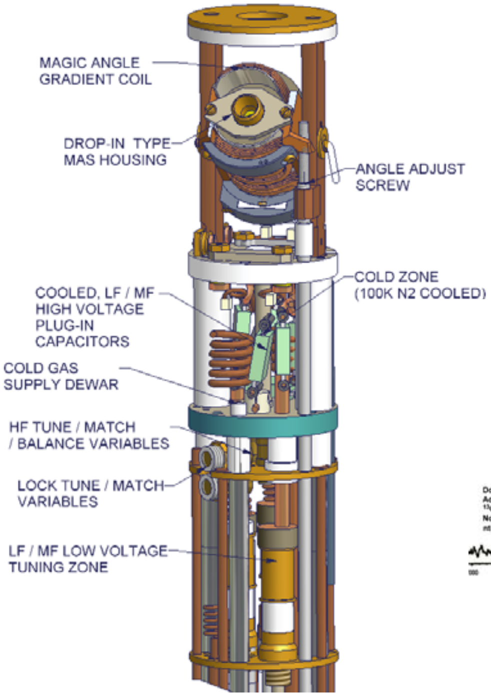

**Figure 5**: 3D view of prototype OptiMAS$^{TM}$ probe, in which the critical circuit components are located in a Cold Zone just below the Spinner Zone (patent pending). Cold nitrogen gas is introduced into this region via a small dewar. Most of this cooling gas exhausts upward, providing some cooling of the flexible leads (not shown) attached to the sample coils but having little effect on the sample temperature, which is primarily established by the bearing gas temperature.

The body tube (not shown) surrounding the probe is a thin-walled metallic dewar, which provides the insulation needed both for the cold zone and extended VT operation.

The variable capacitors are located in RT regions below the cold zone. The unique LF/MF circuit results in the losses associated with the relatively long leads to the variables being only a few percent of sample coil losses, and rf voltages in the tuning zone are low compared to the sample coil voltage to permit maximum LF and MF rf field strengths.

The spinner assembly may be flipped up for automatic sample change. The rotor is caught in a rotor holder at top of the magnet, as seen below in **Figure 6 and 7**.

Figure 6.

Figure 7.

## Building on the Proven XC Advantages

As in most of our solids H/X/Y circuits above 400 MHz, the OptiMAS probe uses a highly optimized cross-coil (XC) for $^1$H and an outer solenoid for the LF and MF channels (see **Figure 3**) because of the strong advantages this approach offers in reducing decoupler heating by an order of magnitude, permitting higher decoupling in high-field MAS, and achieving higher S/N. For example, we have demonstrated S/N greater than 220 on glycine $^{13}$C for H/C/N tuning at 750 MHz – about twice the S/N of alternative solids probes for narrow bore magnets when in the triple configuration.

## Preliminary NMR Test Results

The prototype 300 MHz DI-4 OptiMAS probe was built and tested to verify compatibility with the various features: autosample exchange, multi-nuclear tuning, high power, magic angle gradient (MAG) coil, extended VT, and enhanced S/N using a cold zone. The MAG coil was not included for these, initial tests.

1. The measured gain in S/N for $^{13}$C upon cooling the cold zone to ~90 K was ~83% (compare **Figures 8a and 8b**), which was greater than expected from the simulations.
2. The auto sample exchange mechanism worked very well - though auto control is not yet developed, and a minor change is needed to improve accuracy of the magic angle positioning to a small fraction of a degree.
3. Spinning is exceptionally stable and robust from under 1 kHz to at least 17 kHz at RT, and it appears a different turbine cap design may extend the range to 21 kHz.
4. Sample thermometry needs improvement when the cold zone is cooled, but this should be adequately addressed with a change in the position of the bearing gas thermocouple.
5. The magnetic compensation of the strain reliefs for the flexible leads needs to be improved, as their addition degraded $^1$H resolution from ~0.5 Hz to ~2 Hz.

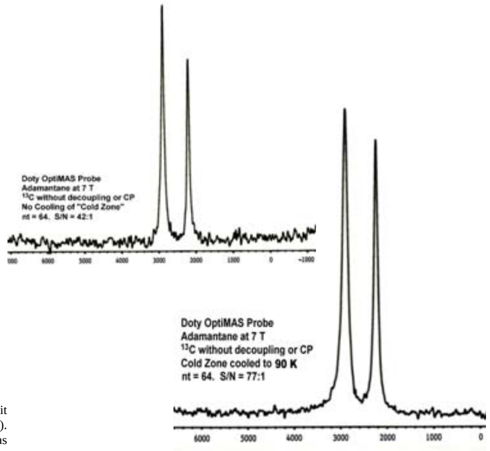

Figure 8a shows $^{13}$C **S/N=42** for the reference case with no cooling of the "Cold Zone".
Figure 8b shows $^{13}$C **S/N=77** with the Cold Zone cooled to ~90 K.

In both cases, no $^1$H decoupling or CP was used – to reduce the uncertainty in quantifying gains in MF S/N. The probe was tuned for H/C/N at 7 T in both cases, and the silicon nitride rotor, filled with adamantane, was spun at ~5 kHz. The cooled $^{13}$C preamp had NF of ~0.2 dB, and the cables, filters, and duplexer added an additional loss of ~0.2 dB ahead of the preamp. The VT controller was not connected, so there was some inadvertant cooling of the sample, which contributed to the higher than expected gain in S/N.

## CONCLUSIONS

Even without cooling of the "Cold Zone", S/N of the OptiMAS probe appears to be higher than reported in alternative "single-coil" designs with auto sample exchange capability (of similar sample size) by ~80% in high-field narrow-bore magnets. Cooling of critical tuning elements to ~90 K, combined with ultra-low-noise preamps and some cooling of the sample coil, permits a further 70-80% increase in S/N in high-performance triple-resonance MAS probes compatible with auto sample exchange, ultra-low rf sample heating, high resolution, and multinuclear tuning at the highest fields.

## REFERENCES

1. F. D. Doty, "Probe Design and Construction," *The Encycl. of NMR Vol. 6*, Wiley, 3753-3762, 1996.
2. F. D. Doty, G. Entzminger, and A. Yang, "Magnetism in HR NMR Probe Design, Part II: HR-MAS, "*Concepts in Magn. Reson.*, (4), 239-260, 1998.
3. F. D. Doty et al, "Reducing Decoupler Heating by an order of magnitude at 750 MHz," presented at the Rocky Mountain Analytical Chem. Conf., Denver, 2004.

**Acknowledgements: This work partially supported by NIH R43 EB00152-02.**